ISSN 2314-5609
Nuclear Sciences Scientific Journal
13, 110-137
2024
https://nssi.journals.ekb.eg

EFFICIENT CLARIFICATION OF INDUSTRIAL HIGH STRENGTH PHOSPHORIC ACID USING MICROWAVE-ACTIVATED CARBON-BASED TIRE WASTE RESIDUE; KINETICS, ISOTHERM, AND THERMODYNAMIC STUDIES

Mahmoud M. El-Maadawy
Nuclear Materials Authority, P.O. Box 530, El Maadi, Cairo, Egypt
E-mail: elma3dawi@yahoo.com

ABSTRACT

This study evaluates the removal of organic matter (OM) from concentrated phosphoric acid as a critical pre-treatment for uranium extraction process. Waste tires were carbonized to produce recovered carbon black particles (AC), which were subsequently activated via microwave treatment (MAC). Both AC and MAC were characterized using FTIR, XRD, Raman spectroscopy, SEM, and BET analysis. OM adsorption experiments were conducted under varying conditions of phosphoric acid concentration, shaking time, temperature, and adsorbent dose. Under optimal conditions (120 minutes, 15 g L^{-1} sorbent, 43% P_2O_5, room temperature), AC achieved a maximum adsorption capacity of 38.46 mg g^{-1}, while MAC reached 47.62 mg g^{-1}. Adsorption kinetics followed pseudo-second-order, with equilibrium data fitting the Langmuir isotherm model. Thermodynamic analysis indicated an endothermic, spontaneous, and feasible adsorption process. This study contributes to improving uranium recovery efficiency from phosphoric acid by addressing organic matter interference. The enhanced OM removal using MAC prepares the phosphoric acid for more effective uranium extraction, potentially increasing yield and purity in subsequent solvent extraction stages, with significant implications for the nuclear fuel cycle and sustainable phosphate resource utilization.

***Keywords*:** Organic matter; adsorption; waste tire; activated carbon; phosphoric acid.

1. INTRODUCTION

Phosphoric acid (PA) is a vital global resource with increasing demand across various industries. Its applications span from fertilizer production, crucial for food security and agricultural productivity, to the manufacturing of detergents, and dental hygiene products (Liu et al., 2022). The growing global population and the need for enhanced crop yields continue to drive the demand for phosphoric acid (Fang et al., 2023). Two primary methods exist for phosphoric acid production: the thermal process and the wet process. The wet process is predominantly favored in industrial settings due to its cost-effectiveness. However, a significant drawback of this process is the contamination of the resulting crude phosphoric acid with substantial levels of organic and metallic pollutants (Fang et al., 2023; Forouzesh et al., 2023). The presence of these contaminants, particularly organic matter (OM), poses significant challenges for both the quality of the phosphoric acid and its potential for uranium recovery. Phosphate rock, the primary raw material for phosphoric acid production, naturally contains trace amounts of uranium. In many cases, the concentration of uranium in phosphoric acid makes its recovery economically viable, presenting an opportunity to supplement uranium supplies for the nuclear fuel cycle while simultaneously purifying the phosphoric acid. However, the organic matter present in crude phosphoric acid significantly impairs the efficiency and yield of uranium recovery (Fang et al., 2023; Forouzesh et al., 2023). These organic compounds interfere with the solvent extraction process commonly used for uranium recovery, reducing extraction efficiency. Furthermore, the presence of OM limits the commercial applicability of phosphoric acid across various industries, necessitating further purification. The complex chemical composition of crude phosphoric acid, makes the purification process both challenging and expensive (Kouzbour et al., 2019). To address these issues, numerous methods have been explored, including reverse osmosis (González et al., 2002), anion-exchange resin(Marszałek et al., 2023), precipitation (Kouzbour et al., 2022), emulsion liquid membrane(Park and Kim, 2021), liquid-liquid extraction(Boulkroune and Meniai, 2012), nanofiltration(Xu et al., 2022), and adsorption (Taha et al., 2014) are operated to clean the yielded phosphoric acid. Among these methods, adsorption has emerged as a particularly promising approach for eliminating pollutants from aqueous solutions. Its advantages include simplicity, affordability, versatility, and minimal waste generation (Morshedy et al., 2021). Activated carbons have gained significant attention as adsorbent materials due to their remarkable capacity to adsorb contaminants, making them a versatile tool for wastewater treatment and purification processes (Tan and Foo, 2022). The efficacy of activated carbons stems from several key characteristics: large inter-particulate surface area, adjustable pore structure, thermo-stability, and modifiable

surface chemistry (Neolaka et al., 2023). However, the high cost of commercial activated carbons has driven research towards more economical alternatives, sparking increased interest in utilizing biomass, bio-based agricultural waste, and similar materials for activated carbon production (Colomba et al., 2022). In this context, tire waste carbon has emerged as an intriguing and cost-effective alternative to commercial activated carbons. Waste tires, which contain approximately 32% carbon by weight, offer a dual benefit: they can be repurposed as an adsorbent material while simultaneously addressing the growing environmental concern of tire waste disposal (Jiang et al., 2023; Joseph et al., 2015). However, carbon obtained from untreated tire pyrolysis typically exhibits a diminished surface area and a less complex pore structure, necessitating appropriate activation to enhance its adsorption performance (Saleh et al., 2013). This study focuses on the production of activated carbons from waste tires and their application in removing organic matter from phosphoric acid as a critical pre-treatment step for uranium extraction. We explore the carbonization of waste tires to produce recovered carbon black particles (AC) and their subsequent activation via microwave treatment (MAC). Microwave activation offers several advantages over traditional heating methods, including faster heating rates, precise control, and the potential for producing activated carbons with fewer oxygenated functionalities on their surfaces (Abderrahim et al., 2023; Ania et al., 2004; Li et al., 2010; Ondon et al., 2014; Thonglhueng et al., 2022).

By investigating the efficacy of these tire-derived activated carbons in OM removal from phosphoric acid, this research aims to address multiple challenges simultaneously: enhancing uranium extraction efficiency, improving phosphoric acid purity for various industrial applications, and contributing to sustainable waste management practices. The study examines the impact of various experimental parameters—such as shaking time, adsorbent dose, phosphoric acid concentration, and temperature—on OM elimination, while also analyzing the mechanism of OM sorption using advanced characterization techniques.

2. EXPERIMENTAL

2.1. MATERIALS:

Abu Zaabal Company for Fertilizers and Chemical Materials provided the high-strength phosphoric acid utilized in the experiment. Table 1 illustrates the chemical composition of the acid as measured using ICP-AES (inductively coupled plasma atomic emission spectrometer, Activa M, Horiba-Jobin Yvon, Longjumeau, France). The activated carbon used in this study was obtained from the discarded tires of vehicles which was sourced from a local company in Cairo, Egypt.

Table 1 Chemical analysis of crude phosphoric acid.

Constituents	Phosphoric acid concentration
Concentration Wt. %	
P_2O_5	≈ 43.0
Fe_2O_3	2.43
CaO	0.46
SiO_2	0.7
F^-	1.3
Concentration (ppm)	
Cd	10
Mn	530
Cu	50
OM	1000

2.2. PREPARATION OF ACTIVATED CARBON

Two steps were involved in the production process of activated carbons: first, the raw waste tires materials were carbonized to produce recovered carbon black particles AC, and then these carbon particles were activated MAC. During the carbonization process, waste tires were broken into pieces and dried in an electric furnace for 24 hours at 110°C to lower their moisture content. These dehydrated tire fragments were heated in a pyrolysis machine to 500°C (Lewandowski et al., 2019) in order to carbonize them and produce black carbon (BC). Following the pyrolysis procedure, BC species were filtered out and then cleaned using organic solvents to remove any remaining organic contaminants. In particular, *n*-hexane was used to wash the BC species, and then a 1:1 by weight mixture of methanol and benzene was applied. With a concentration of 1 g L^{-1} BC in the washing solvents, there was vigorous stirring for 30 min during the washing process. To get rid of any last traces of water, the BC particles were then cleaned with deionized water and dried for an hour at 110°C in a vacuum oven. Lastly, the material was weighed, stored in airtight plastic bags, and consistently referred to as AC throughout the study. The AC was then activated by placing it in a glass reactor inside a microwave oven. The microwave oven was set to an input wattage of 600, and the irradiation time was set to 10 min (Gupta et al., 2014). The resulting sample, was washed with deionized water until the solution reached a neutral pH. After washing, the sample, now known as MAC, was stored for further characterization and adsorption experiments.

2.3. CHARACTERIZATION OF THE PRODUCED CARBONS

Several methods were used to examine the properties of the generated samples, MAC and AC. Scanning electron microscopy (SEM) was used to examine the morphology of the samples, and X-ray diffraction (XRD) was used to ascertain the X-ray diffraction patterns. The KBr technique was used to detect Fourier transform infrared spectrophotometers (FTIRs). Using an integrated microscope (Olympos) and a Raman spectrometer (BRUKER-SENTERRA), the carbon fibre was discovered. Furthermore, a N_2 adsorption-desorption isotherm with a NOVA 3200 apparatus at -196 °C was used to investigate the surface attributes.

2.4. SORPTION METHODOLOGY

The capacity of both carbon samples to adsorb organic materials

from crude phosphoric acid with a commercial concentration of 43% P_2O_5 was assessed using the batch procedure. Thermostatic shaking water baths and plastic containers were used for the experimentation. The study explored the effect of reaction time, dosage amount of addition, and phosphoric acid concentration on the elimination percentage of OM from phosphoric acid. Adsorption experiments were carried out in duplicate, and mean values with relative errors of no more than 3% were considered acceptable for the completed trials. The carbon was removed from the phosphoric acid once equilibrium was attained. A spectrophotometer set at 418 nm was used to measure the amount of organic components present in the crude acid (Ali et al., 2019). The following equations were applied to appreciate the effect of the key variables on the removal efficiency of organic compounds from commercial phosphoric acid:

$$E(\%) = \frac{1 - C_e}{C_o} \times 100 \dots\dots\dots\dots (1)$$

$$q_e = C_o - C_e \times \frac{V}{m} \dots\dots\dots\dots (2)$$

Where C_o and C_e are the organic materials concentration (mg L^{-1}) before the adsorption and at equilibrium, respectively, q_e (mg g^{-1}) is the amount of organic materials sorbet, V is the volume of phosphoric acid (L), and m is the mass of the carbon (g).

3. RESULTS AND DISCUSSIONS

3.1 MATERIALS CHARACTERIZATIONS

3.1.1 FTIR ANALYSIS

A vital method for determining and examining the functional groups like phenols, alcohols, aldehydes, ketones, ethers, carboxyl groups, and carbonyl groups that can bind with OM efficiently in the prepared carbon samples is Fourier Transform Infrared (FTIR) which can bind with OM efficiently (Taha et al., 2019). Figure 1 displays the FTIR spectra of AC and MAC, which serve as adsorbents in the present study. In Figure 1A, a broad band at 3416 cm^{-1}, linked to the O-H stretching modes of the -COOH and phenolic OH groups, is apparent. However, in MAC structure (Figure 1B), this band is less broad and shifted to 3429 cm^{-1}. This discrepancy was most likely caused by the activation procedure using the microwave approach, which reduced the amount of some carboxylic groups. It was possible to identify the C-H bond peak, which ranges from 3000 to 2800 cm^{-1}, in both carbon architectures. As a result of the activation process, the measured peak in the case of MAC was slightly shifted, but it still show off significant variations in form or intensity. This data suggests that the process of producing activated carbon species did not degrade the hydrocarbon backbone of the blank carbon through microwave irradiation. In contrast, significant differences were evident in the FTIR spectra, ranging from 1650 to 1000 cm^{-1}, upon comparing the two structures. Within the AC, four bands corresponding to C-O, S-O-C, C-O-C, S=O, and C-C bonds were noticeable. However, there was a decrease in the number of these peaks, leading to the emergence of two

broader absorption bands, which suggests the merging of the former four peaks in the activated carbon sample. These alterations can be attributed to the structural chemical changes occurring during the activation process, which lead to the creation of sulfonyl groups such as sulfone (-R-SO_2-R-) and sulfoxide (R-S=O) (Aoudia et al., 2017). These results verify that during microwave usage, oxidative breakdown of the main chain occurred simultaneously with rubber devulcanization. Furthermore, in the case of AC, FTIR bands corresponding to C-S and S-S bonds were discernible between 400 and 650 cm^{-1}. Conversely, these bands vanished in the activated carbon sample, indicating that the preparation processes using microwave treatment broke a significant amount of the vulcanization linkages (Aoudia et al., 2017). This clearly indicates the substantial impact of the oxidative process during the transformation of carbon black into the activated carbon structure.

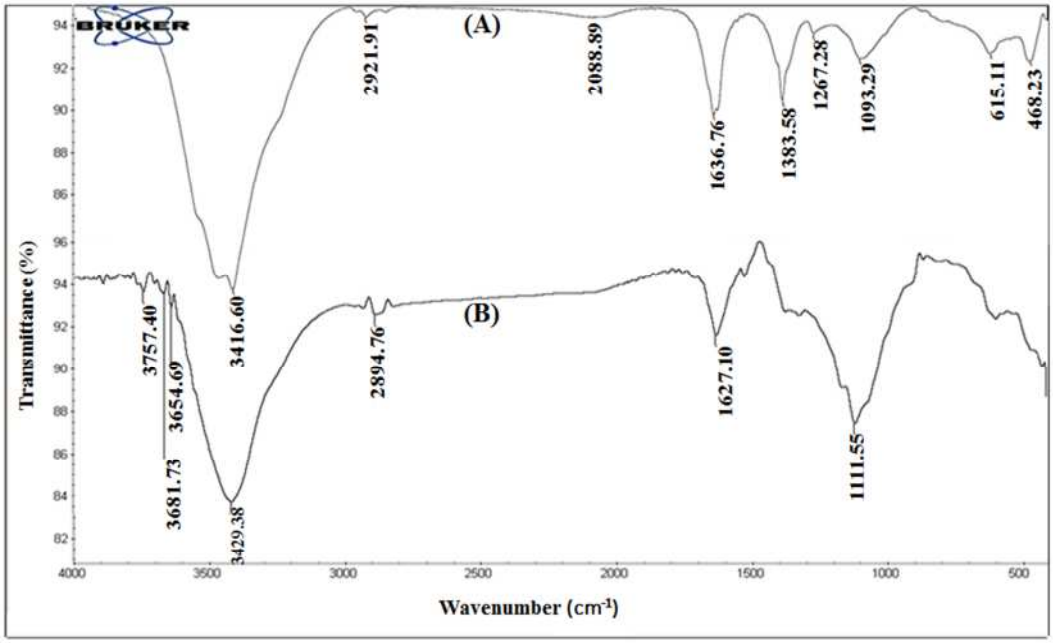

Fig. 1: FT-IR spectrums of (A) AC (B) MAC carbon species.

3.1.2 BET

Table 2 displays the results of applying the BET method to determine the surface properties of two samples. The BET-specific surface area of the activated carbon (MAC) was about double that of the blank carbon black (AC). On the other hand, compared to (MAC), the total pore volume of (AC) was somewhat lower. Mesoporous were discovered to be present in both structures, however (MAC) exhibited narrower mesoporous than (AC). The explanation for these variations in surface properties can be found in the reconstruction and rearrangement of (MAC) species that occur during the microwave processing phase.

Table 2: surface characteristics of AC and MAC carbon species.

Sample	Surface Area	Total Pore Volume	Average Pore Size
AC	52 m^2g^{-1}	0.40 ccg^{-1}	31 nm
MAC	96 m^2g^{-1}	0.45 ccg^{-1}	18 nm

3.1.3 RAMAN ANALYSIS

The vibrational properties of sp2-hybridized carbons have been investigated using Raman spectroscopy, which has provided valuable insights into the sp2-sp3 hybridization ratio (El-Maadawy et al., 2024). The D band and G band are two characteristic properties of carbon-based materials. All graphite-like carbons exhibit the D band, sometimes referred to as the disorder or defect band, which is a sign of structural faults since it originates from a hybridised vibrational mode connected to carbon edges (Chailuecha et al., 2021). Moreover, the "turbostratic carbon structure" is another name for the D band.(Morshedy et al., 2021). Conversely, the graphitization level is described by the G band (1595 cm^{-1}) (Raimundo et al., 2022) is the result of the stretching mode in the C-C bond found in graphitic materials as well as the hybridization of carbon (sp2) (Poursorkhabi et al., 2020). Two bands with relatively similar intensities, the D band at 1388 cm^{-1} and the G band at 1565 cm^{-1}, are visible in The spectrum of the MAC sample, displaying the distinctive characteristics of carbon compounds (Chaudhuri et al., 2022). On the other hand, the AC sample showed a substantially stronger vibrational mode (D band) at 1334 cm^{-1} than the G band (Liu et al., 2008). In contrast to MAC, the amorphous and disordered structure of AC is implied by the presence of such a prominent D band. This is because the intensity of the D band and the crystalline structure have an inverse connection when the Raman k-selection rule is broken. One often used metric to assess the degree of structural disorder in carbon materials is the I_D/I_G ratio. It is calculated by dividing the Raman-allowed band's integrated intensity by the integrated intensity of the disorder-induced band (Morshedy et al., 2021). This ratio is a frequently used metric for evaluating structural order since it estimates the quantity of edge plane exposure and indicates the number of structural flaws (Liu et al., 2008). It is commonly known that a higher I_D/I_G ratio is linked to a carbon structure with a higher degree of flaws (Taha et al., 2019). For MAC, the I_D/I_G ratio is somewhat less than 1, but for AC, it is much more than 1. This demonstrates unequivocally that, in contrast to AC, the structure of MAC is more strongly crystalline and organized (Qu et al., 2018).

3.1.4 SEM

Figures 3a and 3b display the SEM micrographs of AC and MAC, respectively. As seen in Figure 3a, AC has a wavy morphology, a slightly porous structure, and tiny pores that vary in size and shape. Conversely, the MAC depicted in Figure 3b has a little more porous structure and a smoother surface. This suggests that the activation process using microwaves enhanced the surface appearance of raw carbon. The surface area analysis and the greater porosity of the activated carbon are consistent, as evidenced by the homogeneous distribution of regularly formed pores and many cavities. This unequivocally confirms the potential of MAC as a highly effective adsorbent, a

conclusion that can be confidently drawn.

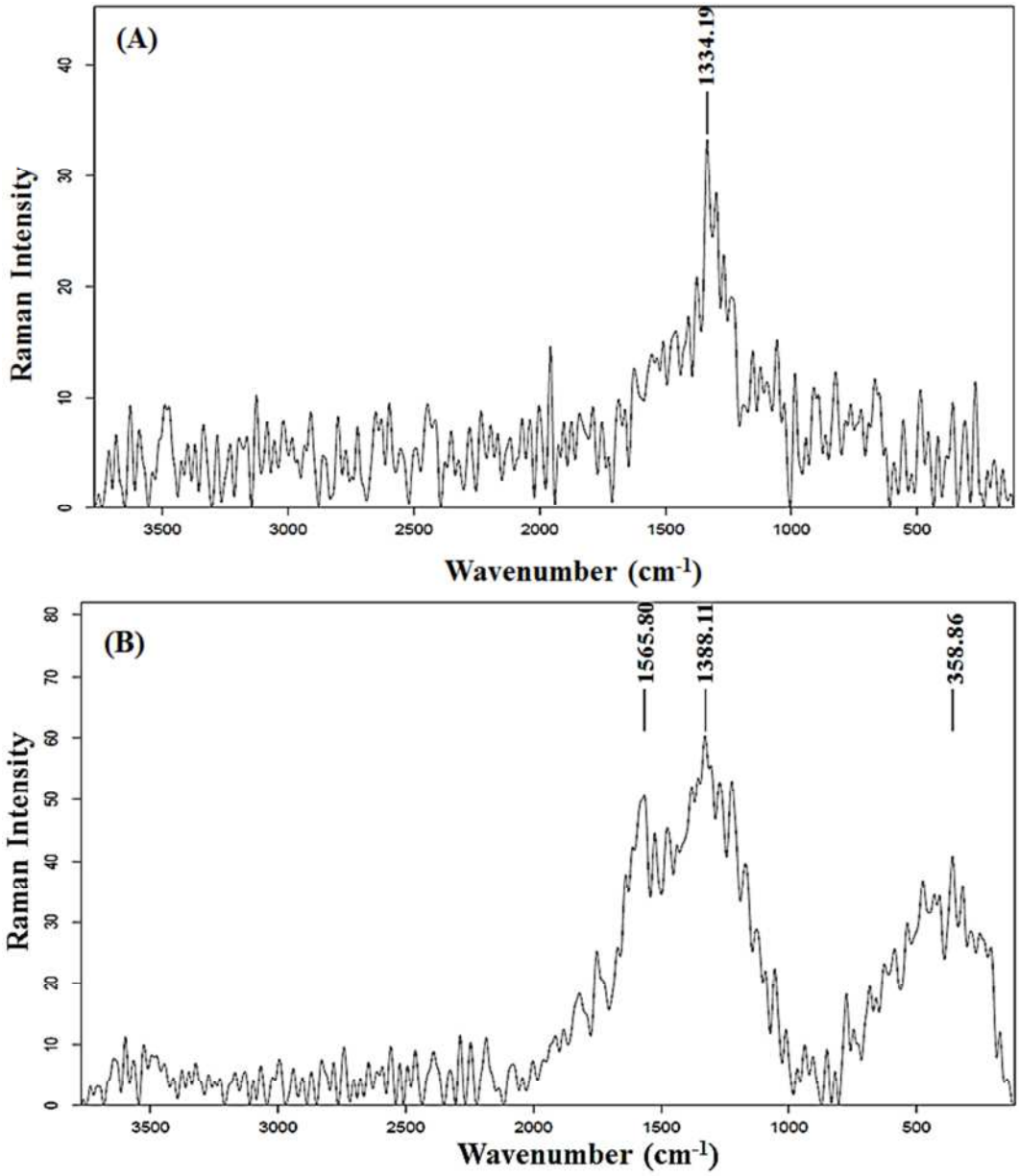

Fig. 2: Raman analysis of (A) AC (B) MAC species.

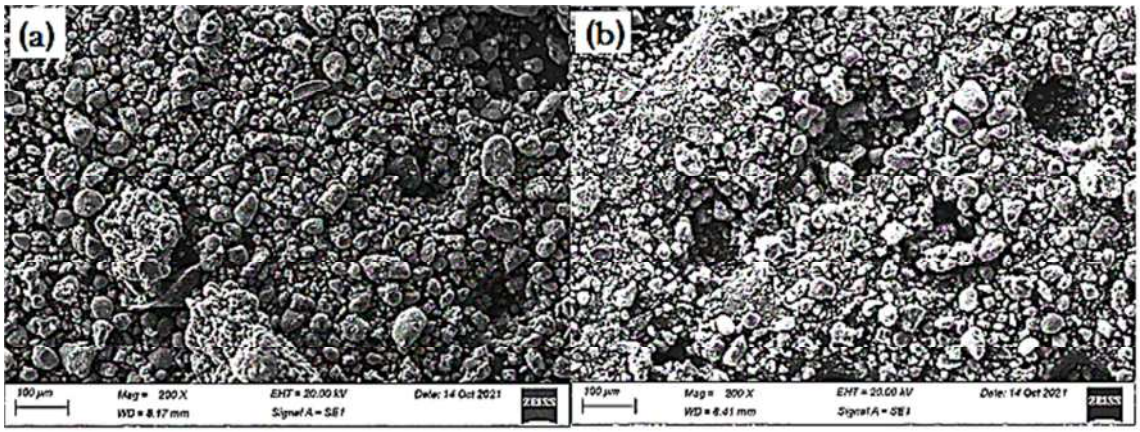

Fig. 3: morphological appearance of (a) AC (b) MAC species.

3.1.5 XRD ANALYSIS

A method used to determine the crystalline structure of a compound is X-ray diffraction (XRD) (Chaudhuri et al., 2022). The XRD spectra of the AC and MAC are shown in Figure 4 so that their structural properties can be examined. The large peak that both samples exhibit between 15° and 39° can be attributed to their amorphous carbon structure. But, MAC is less broad and has a lot of abrupt peaks, which suggests that it is a mixed structure with both amorphous and crystalline elements. Two peaks are also visible in the XRD patterns, at approximately 26.78° and 42.17°, which correspond to the amorphous carbon reflection lattice planes (002) and (101). According to Poursorkhabi et al.,(Poursorkhabi et al., 2020) these peaks are typically attributed to the graphitic structure and are typical of carbon-based material.

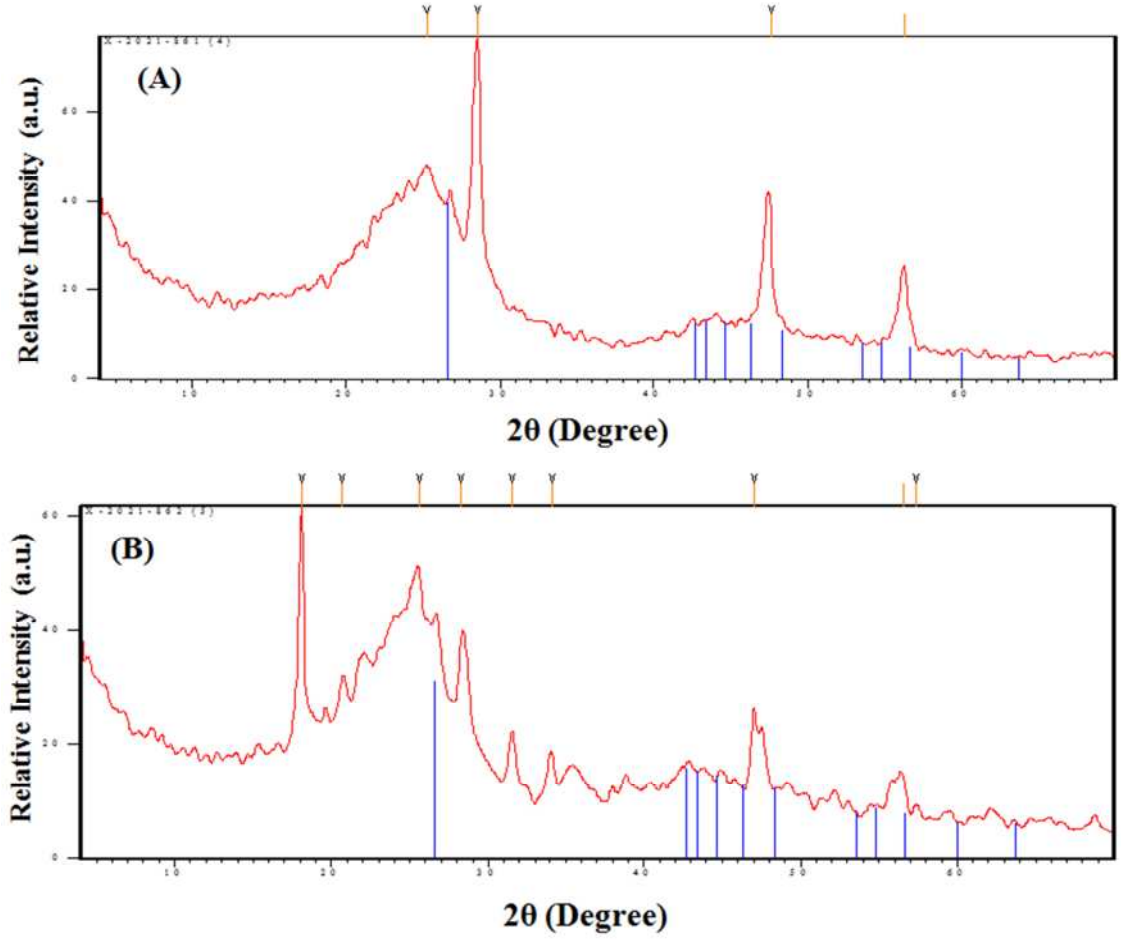

Fig. 4: XRD patterns of (A) AC (B) MAC species.

3.2. SORPTION INVESTIGATION

This section is devoted to the purification of commercial phosphoric acid using two carbon waste materials: AC and MAC. The goal is to produce an acid that is appropriate for use in the manufacturing of pure fertilizers. This study examines the effects of temperature, phosphoric acid concentration, shaking time, carbon dosage, and temperature on the percentage of organic component adsorption. This paper also contains assessments of sorption isotherms, kinetics, and thermodynamics, which offer important information required

for process design and scaling-up experiments.

3.2.1. EFFECT OF SHAKING TIME

Using two distinct types of carbons, AC and MAC, several tests were carried out to investigate the effect of reaction time (between 5 and 600 min) on the sorption of organic species from crude phosphoric acid (43%). During these tests, each type of carbon was mixed with phosphoric acid at a sorbent dose of 15.0 g L^{-1}, with a shaking speed of 150 rpm, and conducted at room temperature. The proportion of organic compound adsorption as a function of shaking time is displayed in Figure 5. The findings show that both carbon types quickly reach equilibrium in the process of absorbing organic molecules from commercial phosphoric acid; for both sorbents, this equilibrium is reached after 120 min. Furthermore, the two sorbents operate similarly in terms of absorption. There are two steps to the sorption reaction: the first stage and the second stage. There is a high rate of adsorption during the first phase, which lasts for 1 to 120 min. The sorption efficiency of the organic compounds rose during this period, rising from 11.3% to 53.3% for AC and from 17.4% to 71.6% for MAC. The existence of vacant active sites on the surface of the carbon could be the cause of this behaviour (Taha et al., 2018). The second stage is marked by a gradual reaction rate, during which the sorption percentage of OM marginally increases. When the shaking duration is increased from 120 to 600 minutes, it climbs from roughly 53.3% to 56.0% for activated carbon AC and from 71.6% to 73.7% for MAC (El-Maadawy, 2019). This behavior might be explained by the fact that most of the sorbent surface active sites are already in use, which gives the molecules of OM more time to diffuse and react with the interior active groups. This result is in line with earlier studies (Masoud et al., 2020). The investigations that followed were carried out at 120 minutes to confirm that total equilibrium had been established.

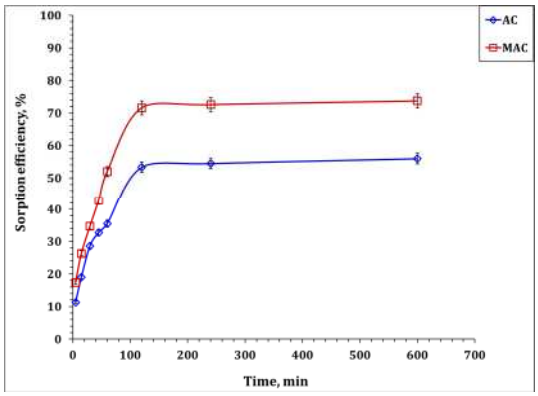

Fig. 5: The variation of OM sorption as a function of shaking time

3.2.2. INFLUENCE OF PHOSPHORIC ACID CONCENTRATION

AC and MAC sorbents were used in a series of experiments to examine the impact of phosphoric acid concentrations ranging from 20% to 43% on the sorption of OM. The experiments were conducted at a temperature of 25 ± 1°C, with a reaction duration of 120 minutes and a stirring speed of 150 rpm. Figure 6 presents the test data and illustrates the correlation between the percentage of sorption of OM and the percentage of phosphoric acid. The findings show that the two sorbents responded to an increase in phosphoric acid content in a comparable way. In particular, as the

concentration of phosphoric acid increased from 20% to 43%, the sorption efficiency of OM decreased dramatically, going from 78.9% to 55.1% for AC and from 85.9% to 71.2% for MAC. The reason behind this behavior is that when the concentration of phosphoric acid rises, more phosphoric acid molecules are produced. This leads to an increased amount of extra acid molecules covering the surface active sites of the sorbent particles. As a result, this reduces the sorption capability for sorption. Furthermore, an increase in acid molarity raises the acid bulk density, which adversely affects the ability of OM to diffuse to the sorbent surface (Leydier et al., 2017).

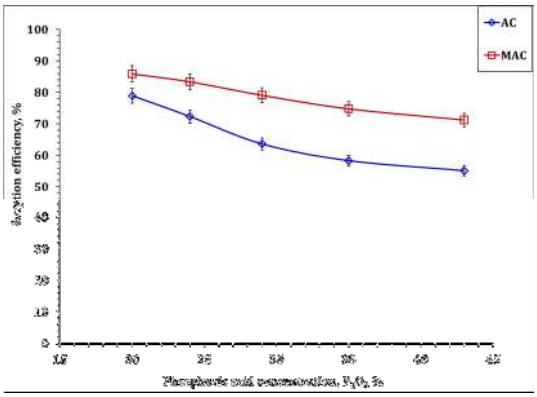

Fig. 6: OM sorption efficiency as a function of phosphoric acid concentration.

3.2.3. EFFECT OF SORBENT DOSE

The impact of AC and MAC on the reduction of OM in commercial phosphoric acid is examined in Figure 7. The investigation examined sorbent dose between 8 and 20 g L^{-1} while maintaining constant parameters such as room temperature, a phosphoric acid concentration of 43%, a stirring speed of 150 rpm, and a shaking duration of 120 minutes. The findings demonstrated that because there were more active reaction sites available, raising the sorbent dose increased the percentage of OM that were adsorbed (Beltrami et al., 2013). The sorption of OM increased from 31.2% to 69% for AC and from 42% to 88% for MAC sorbents as the carbon dose increased from 8 to 20.0 g L^{-1}. As the sorbent dose increased, the sorption capacity (qe) of the waste carbon sorbents diminished, with the qe value declining from 33.9 to 30 mg g^{-1} for AC and from 45.7 to 38.3 mg g^{-1} for MAC. This phenomenon may be ascribed to the constrained availability of active sites on the sorbent for the binding of organic compound molecules, along with the inadequate concentration of organic compounds to saturate the sorbents' adsorption capacities, thereby resulting in a decrease in the qe value (Liu et al., 2008; Morsy et al., 2019).

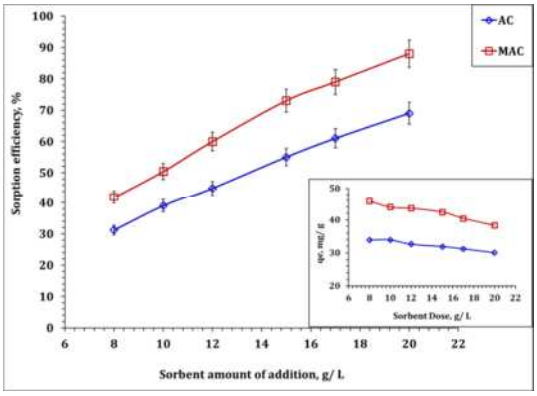

Fig. 7: OM sorption efficiency as a function of sorbent amount of addition.

3.2.4. EFFECT OF TEMPERATURE

Within a 25–50 ^{o}C range, the study sought to investigate how temperature affected the purification of phosphoric acid from OM using AC and MAC. The operating parameters were a 43% concentration of

phosphoric acid, 15 g L^{-1} of adsorbent, 150 rpm of stirring speed, and 120 minutes of shaking duration. Figure 8 illustrates how the amount of adsorption somewhat increased as the temperature rose, suggesting that the process was endothermic. Furthermore, it was discovered that the removal of each metal ion was more advantageous at higher temperatures, which is in line with many researches (Sultana et al., 2022). The vibration of the molecules in the reaction media, which blocks the active sites, may be the cause of the increase in adsorption with temperature (Semião et al., 2010).

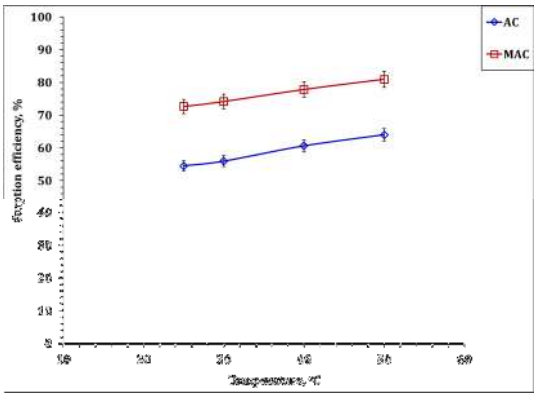

Fig. 8: OM sorption of as a function of solution temperature

3.3. THE UPTAKE KINETICS

The uptake kinetics of solid-liquid reactions must be investigated in order to have a better understanding of the rate at which reactions take place and the functioning of adsorption processes. The kinetics of OM removal from industrial phosphoric acid utilizing waste carbon from AC and MAC processes are the main focus of this work. Three kinetic models Lagergren, pseudo-second-order, and Weber and Morris kinetic model were used to analyze the adsorption data (El-Maadawy, 2024; Elgohary et al., 2024; Ibrahim et al., 2024; Masoud et al., 2024; Youssef et al., 2024). These models are shown in Figures 9–11 and are represented by equations (3), (4), and (5). Table 2 contains a list of the generated kinetic model constants. Which kinetic equation best captures the interaction between the materials and OM was found using the coefficient of correlation (R^2).

$$\log\left(q_e - q_t\right) = \log q_e - \frac{k_1}{2.303} t \quad \text{.....(3)}$$

$$\frac{t}{qt} = \frac{1}{k_2 q_e^2} + \frac{1}{q_e}(t) \quad \text{.....(4)}$$

$$q_t = K_{id} t^{0.5} + C \quad \text{..... (5)}$$

Where qt and qe are the amounts of OM adsorbed (mg g^{-1}) at time t (min) and at equilibrium, respectively; k_1 (min^{-1}), k_2 (gmg^{-1} min^{-1}), and K_{id} (mg g^{-1}. $min^{-0.5}$) are the sorption rate constant of Lagergreen, the pseudo-second-order, and Weber-Morris kinetic models, respectively; C is the thickness of the boundary layer.

As shown in Figure 9, the pseudo-first-order equation has been used to evaluate the experimental data. It is clear from the figure that the relationship between Log(qe-qt) vs. time produces straight lines with a low correlation coefficient, indicating that the sorption process of OM does not fit the Lagergren equation well. The Lagergren kinetic model is only useful for characterizing the first stage of sorption processes, and it frequently does not fit well for the entirety of reaction times in the literature (Heidarinejad et al., 2020). The pseudo-second-order reaction equation was used to analyses the findings, as seen in Figure 10. With a correlation coefficient of 0.99, the relationship between t/qt and sorption time was

found to be linear, demonstrating that the equation provided a good fit for both carbon materials under test. Furthermore, the calculated sorption capacity (qe cal) and experimental sorption capacity (qe exp) for AC and MAC sorbents matched, indicating that the pseudo-second-order kinetic equation is a useful tool for characterizing the OM sorption from crude phosphoric acid using carbons from AC and MAC. Thus, evidence for a chemisorption mechanism participating in the organic matter sorption process is presented(Ali et al., 2019; Taha et al., 2019); Appropriate clarification should be provided regarding the thermodynamic parameters of the sorption process(Taha et al., 2018). According to earlier studies, the presence of surface functional groups on the applied waste carbon sorbents may improve electron transfer or sharing with organic contaminants (Ali et al., 2019; Taha et al., 2019).

The pseudo-second-order kinetic model describes the sorption process of OM, which is a chemisorption reaction. However, the mechanism of OM adsorption cannot be clearly explained by this model. Sorption kinetics in solid-liquid reactions can be controlled by a variety of diffusion processes, including resistance to bulk diffusion, film diffusion, and intraparticle diffusion. The resistance to film diffusion is initially active when liquid phosphoric acid and carbon sorbents are mixed. However, the impact of resistance to bulk diffusion can be disregarded if enough velocity is used to combine the phosphoric acid and carbon sorbents. Consequently, the primary regulating step becomes the resistance to intraparticle diffusion. The Morris-Weber model was used to analyze the experimental results, as Figure 11 illustrates. Table 3 displays the values of the model constants that were determined by examining the plot of qt with respect to time. Figure 11 illustrates two distinct regions exhibiting a multi-linear relationship for both AC and MAC sorbents. This suggests that the sorption mechanism of OM is not exclusively governed by intraparticle diffusion. Varied transfer rates of OM molecules may exist between the initial and final sorption stages, thereby mitigating the boundary layer effect (Şenol and Şimşek, 2020).

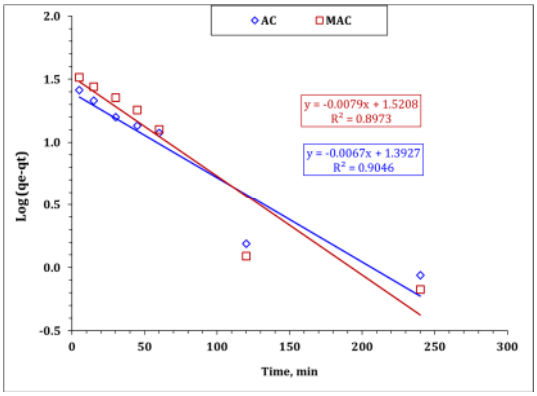

Fig. 9: Lagergreen kinetic model plot for OM adsorption

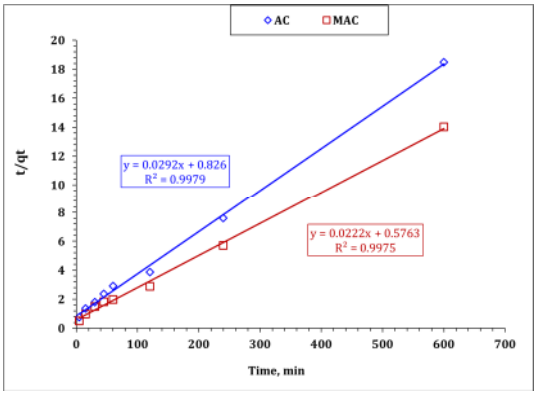

Fig. 10: Pseudo second-order kinetic model plot for OM adsorption

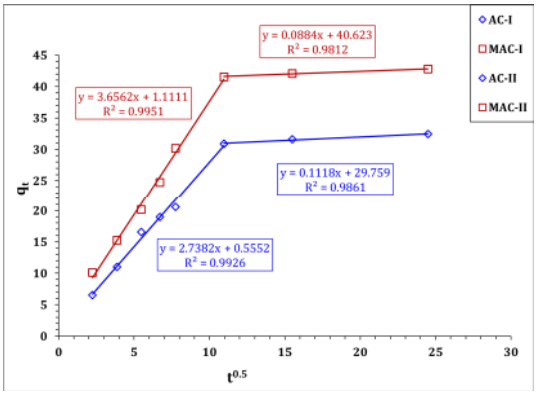

Fig. 11: Weber and Morris kinetic model plot for OM adsorption

Table 3 demonstrates that for the two sorbents employed, a low boundary layer effect and a high sorption rate are indicative of the first stage of the OM adsorption process. This attests to the quick response. The existence of surface active sites, which cause external surface adsorption (Şenol and Şimşek, 2020). Conversely, a higher boundary layer impact for AC and MAC carbon and a lower absorption rate characterize the second stage. This could be because intraparticle diffusion is caused by the saturation of most carbon surface sites. Thus, it can be deduced that the combination of external surface adsorption and intraparticle diffusion as rate-controlling stages regulates the sorption of OM from commercial phosphoric acid utilizing AC and MAC carbon (Taha et al., 2019).

Table 3: The evaluated parameters of the kinetic models

		AC	MAC
Lagergreen pseudo first-order	k_1 (min $^{-1}$)	0.015	0.018
	qe_{cal} (mgg^{-1})	24.7	33.2
	qe_{exp} (mgg^{-1})	32.5	42.8
	R^2	0.90	0.89
Pseudo second-order	k_2 (min $^{-1}$)	0.001	0.001
	qe_{cal} (mgg^{-1})	34.2	45.0
	qe_{exp} (mgg^{-1})	32.5	42.8
	h (mol g^{-1} h^{-1})	1.21	1.74
	$t_{1/2}$ (h)	28.3	26.0
	R^2	0.99	0.99
Weber and Morris model	**Stage I**		
	k_i (mgg^{-1} min$^{1/2}$)	2.74	0.56
	C	0.6	29.8
	R^2	0.99	0.98
	Stage II		
	k_i (mgg^{-1} min$^{1/2}$)	3.66	0.09
	C	1.1	40.6
	R^2	0.99	0.98

3.4. SORPTION ISOTHERM:

The relationship between the solute concentration in the aqueous phase and the solid phase at a specific temperature is represented by the adsorption isotherm(Badr et al., 2023; Masoud et al., 2020; Masoud et al., 2023; Youssef et al., 2022). Examining the isotherm yields vital information

for process optimization and system scalability. The standard models used to explain the uptake of OM using AC and MAC carbons from commercial phosphoric acid are the Freundlich and Langmuir isotherm models. The Freundlich isotherm model primarily describes heterogeneous adsorption systems and is not restricted to the monolayer sorption process. Conversely, the Langmuir isotherm model is limited to monolayer and homogenous adsorption systems (Azizian and Eris, 2021; Shekhawat et al., 2023). The linear forms of the Freundlich and Langmuir models are represented, respectively, by equations 6-7.

$$\log q_e = \log K_F + \frac{1}{n}\log C_e \ldots Eq\ (6)$$

$$\frac{C_e}{q_e} = \frac{1}{bQ_o} + \frac{C_e}{Q_o} \ldots\ldots Eq\ (7)$$

Where K_f (mg g^{-1}) is the adsorption capacity; Q_m (mg g^{-1}) is the monolayer adsorption; b (L mg^{-1}) and 1/n are Langmuir and Freundlich constants respectively; R_L the separation factor and calculated by $R_L = 1/(1 + k_L C_o)$.

The Freundlich isotherm parameters can be assessed by plotting log qe against log Ce (Figure 12), whereas the relationship between Ce/qe versus Ce (Figure 13) can be utilized for evaluating Langmuir isotherm variables. The estimated isotherm variables are presented in Table 4. The isotherm outcomes indicate that the sorption of OM conforms well to the Langmuir isotherm model, as it exhibits the highest correlation coefficient (R^2 = 0.99) for both applied sorbents. This observation suggests a monolayer and homogeneous sorption process (Azizian and Eris, 2021; Largitte and Pasquier, 2016; Martínez et al., 2023; Shekhawat et al., 2023). However, the Freundlich plot (Figure 12) displays a strong linear relationship ($R^2 \approx 0.97$), suggesting a possibility of a heterogeneous adsorption process, although with a limited contribution (Azizian and Eris, 2021; Şenol and Şimşek, 2020). The adsorption of organic contaminants from industrial phosphoric acid was observed to follow the same isotherm profile (monolayer and homogenous process) (El Naggar et al., 2019).

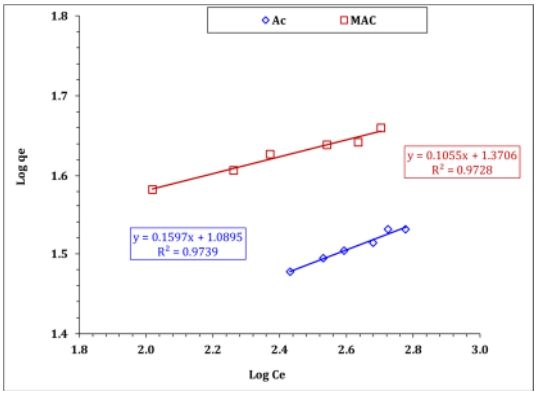

Fig. 12: Freundlich model plot for OM adsorption

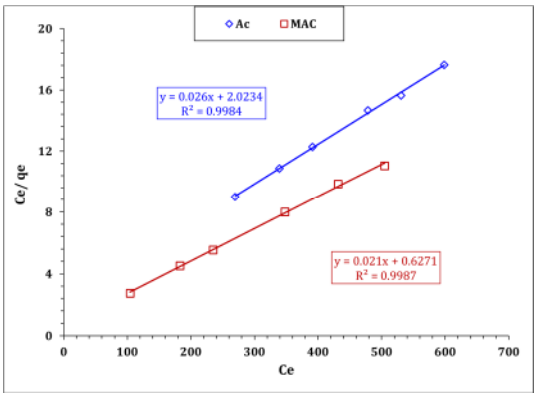

Fig. 13: Langmuir model plot for OM sorption.

Table 4: The evaluated variables of isotherm models

		AC	MAC
Freundlich isotherm model	**n**	6.26	9.48
	K_f (mg/ g)	12.29	23.47
	R^2	0.97	0.97
Langmuir isotherm model	**Q_m (mg/g)**	38.46	47.62
	b (L/ mg)	0.013	0.970
	R_L	0.082	0.001
	R^2	0.99	0.99

Comparative studies have been conducted between the adsorption capacities of AC and MAC carbon sorbents and other adsorbents utilized for the same purpose. Table 5 presents the findings. The results verify that AC and MAC possess a noteworthy capacity for sorption of organic substances, which is in line with other sorbents reported in the literature. As a result, crude phosphoric acid can be efficiently clarified using these carbons.

THERMODYNAMICS:

In order to describe the sorption behavior and system scaling up, thermodynamic parameters like Gibbs free energy change (ΔG^o), standard enthalpy change (ΔH^o), and standard entropy change (ΔS^o) are essential. The thermodynamic performance of OM sorption employing carbons AC and MAC was examined using equations (8–10) (Doke and Khan, 2012; Jin et al., 2018):

Table 5: Comparison of sorption performance of OM for different sorbents.

Sorbent	Qm, mg g^{-1}	Ref
Blank bio-char	33.6	(Taha et al., 2019)
Hydrochloric acid activated bio-char	53.7	
Nitric acid activated bio-char	47.9	
Sludge El Sheikh Zaid	22.8	(Ibrahim et al., 2021)
Sludge Al Obour	23.3	
Sludge El Marq	26.3	
Natural bentonite	24.0	(Ali et al., 2019)
Sulphuric acid activated bentonite	27.7	
Nitric acid activated bentonite	17.3	
Hydrochloric acid activated bentonite	8.6	
Carbon AC	**38.4**	**Present Work**
Carbon MAC	**47.6**	

3.5. SORPTION THERMODYNAMICS:

$$\log k_C = -\frac{\Delta H^o}{2.303R} X \frac{1}{T} + C \ldots (8)$$

$$-\Delta G^o = 2.303RT \log k_C \ldots (9)$$

$$-\Delta G^o = \Delta H^o - T\Delta S^o \ldots (10)$$

Where K_C is a non-dimensional equilibrium constant (K_C = K_d X ρ X 1000) (Morsy et al., 2019; Sultana et al., 2022); T is the temperature (K), R is the universal gas constant (8.314 J $mol^{-1}.K^{-1}$), ρ is the solution density (g L^{-1}), and C is a constant.

One way to assess the thermodynamic variables of the sorption process is with the Van't Hoff

plot (Figure 14). Table 6 presents the findings. The negative ΔG^o values in the data show that the sorption process utilizing the AC and MAC sorbents is possible and spontaneous (Cordova Estrada et al., 2021). The reaction becomes more possible as the temperature of the reaction rises because the ΔG^o values become more negative. The sorption of OM is endothermic, as evidenced by the positive ΔH^o values (12.99 kJ/mol) of the manufactured carbons, MAC and AC. The positive values of ΔS^o (83.4 J/mol K for AC and 90.03 J/mol K for MAC) indicate an increase in randomness at the solid-liquid interface during OM sorption (Martínez et al., 2023). A similar thermodynamic profile was observed for the removal of OM from commercial phosphoric acid using activated bentonite (Ali et al., 2019).

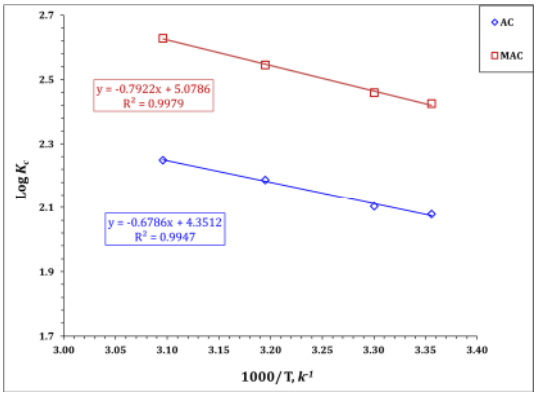

Fig. 14: Van't Hoff equation plot for OM sorption

Table 6: Thermodynamic variables for OM sorption

	ΔG (kJ/ mol)				ΔH	ΔS
	20 °C	30 °C	40 °C	50 °C	(kJ/ mol)	(J/ mol K)
AC	-11.86	-12.21	-13.11	-13.91	12.99	83.40
MAC	-13.83	-14.27	-15.26	-16.25	12.99	90.03

3.7. REUSABILITY OF ACID ACTIVATED BIO-CHAR

The MAC-activated carbon sorbent underwent a hot distilled water wash and was reused for adsorbing organic matter (OM) from crude high-strength phosphoric acid. The reusability of MAC was evaluated by repeating this process multiple times. Figure 15 illustrates the reusability efficiency of MAC for OM adsorption. The results indicate that the MAC retained a large portion of its efficiency after five consecutive cycles. This suggests that MAC can effectively undergo five consecutive adsorption and desorption cycles.

Subsequently, the carbon undergoes a microwave activation process. Taking into account the number of adsorption-desorption cycles and the energy consumption during the preparation of carbon materials, the carbon structures presented are highly suitable for this application. Carbon production via the microwave process can be achieved with an irradiation time of 10 minutes and a power input of 600 (Ania et al., 2004). Hence, the energy consumption during the carbon synthesis step is significantly lower compared to conventional heating techniques. This offers economic advantages when utilizing such adsorbents for industrial phosphoric acid purification.

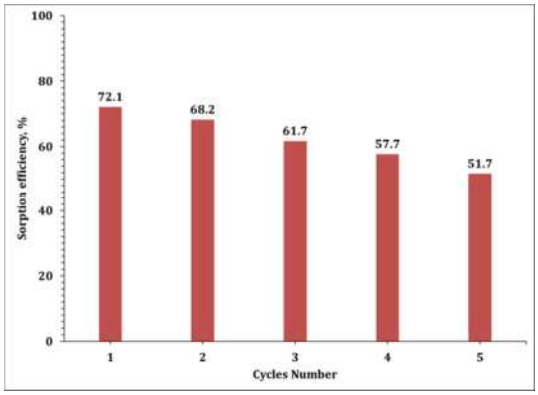

Fig. 15: The number of cycles for the applied MAC sorbent.

3.6. DEVELOPED PHOSPHORIC ACID PRE-TREATMENT FOR PROCESS SCALE UP

According to a study on the use of MAC carbon for industrial phosphoric acid purification, this sorbent demonstrated the high level of efficiency. The best experimental conditions were found to be room temperature, 120 minutes for the reaction, and 15 g L^{-1} of sorbent. Utilizing these conditions, a process was formulated for clarifying industrial high-strength phosphoric acid (≈43.0% P_2O_5) using MAC sorbent. Table 7 displays the chemical properties of the resultant phosphoric acid. According to the study, MAC sorbent successfully lowered the concentration of OM by 72% while also lowering the iron ion content of the crude phosphoric acid by roughly 11%. This suggests that the sorbent that has been prepared can be utilized to efficiently clarify crude phosphoric acid, resulting in the creation of phosphate fertilizers that are environmentally beneficial.

Table 7: Chemical analysis of crude and treated phosphoric acid.

Constituents	Phosphoric acid	
	Before	After
Concentration Wt. %		
P_2O_5	≈ 43.0	≈ 43.0
Fe_2O_3	2.43	2.15
CaO	0.46	0.45
SiO_2	0.7	0.7
F^-	1.3	1.3
Concentration (ppm)		
Cd	10	3.8
Mn	530	461
Cu	50	28.5
OM	1000	280

3.7. MECHANISM OF ORGANIC MATTER ADSORPTION PROCESS:

To enhance the sorption process, it is important to comprehend how different organic matter species interact with MAC (Hamza et al., 2020, 2013). OM/MAC interaction may entail multiple types of interactions, including as physical adsorption, hydrogen bond formation, complex creation, electrostatic attraction, and π-π interactions (Abderrahim et al., 2023; Hamza et al., 2020, 2013). While they are regulating the size and surface charge of OM molecules, ionic strength, divalent metal ion concentration, and solution pH are significant factors in OM adsorption from aqueous solution (Abderrahim et

al., 2023; Hamza et al., 2020, 2013; Ibrahim et al., 2021).

As far as the author is aware, organic compounds found in wet phosphoric acid include aromatics, humic compounds, and a range of saturated and unsaturated fatty acids, such as butylated hydroxytoluene (2,6-Di-tert-butyl-4-methylphenol), azelaic acid (Bis [tert-butyl(dimethyl)silyl] azelaate), and dibutyl phthalate (Ali et al., 2019; Fawzy et al., 2018; Ibrahim et al., 2021; Jjagwe et al., 2021; Mohamad Nor et al., 2013). Furthermore, there is a large concentration of cations in wet phosphoric acid, especially multivalent cations like Ca(II), which help adsorb (OM) by neutralizing its charge and shrinking its size. Consequently, there is an increase in the collection of OM molecules on the activated carbon surface that has been applied (Abderrahim et al., 2023; Awwad et al., 2013; Doke and Khan, 2012; Fawzy et al., 2018; Hamza et al., 2013; Jjagwe et al., 2021; Mohamad Nor et al., 2013).

In this work, we contrasted waste tire-derived AC with MAC. The MAC has a higher surface area (52 m^2 g^{-1} and 96 m^2 g^{-1} for AC and MAC, respectively) and a more porous structure (as shown in Figure 3), indicating that the microwave activation process improves the sorption characteristics of the applied sorbents. The two carbon compounds have identical chemical structures. The results of kinetic and isotherm analyses point to a chemisorption process for the adsorption of organic matter (OM), with an electron exchange between the OM species and the added sorbent serving as the rate-limiting phase. This implies that a surface complexation mechanism between the OM species and the surface active functional groups (such R-S=O, C-O-C, and C-S) on the applied AC and MAC may be in charge of the sorption process.

Several reaction mechanisms clearly govern the OM adsorption process in the Weber-Morris kinetic model study. Hydrogen bond formation and π-π interactions between OM species and the sorbent surface function groups may transpire during the sorption process. According to research by Ando and his colleagues, the physical adsorption process regulates the uptake of OM, suggesting a direct relationship between the sorbent surface area and sorption ability (Ali et al., 2019). This implies that the sorption capacity for OM will be higher for the sorbent with a larger surface area and pore structure. This is consistent with the experimental results, where MAC demonstrated a higher sorption capacity (47.62 mg g^{-1}) than AC (38.46 mg g^{-1}), confirming that the activation process improves the sorption characteristics of the prepared carbon from tire waste.

CONCLUSION

This study demonstrates the effective separation of organic matter

(OM) from crude phosphoric acid (43% P2O5) using activated carbons derived from waste tires (AC and MAC). The microwave-activated carbon (MAC) showed superior performance in OM removal, achieving an adsorption capacity of 47.63 mg g^{-1} compared to 38.4 mg g^{-1} for AC. Both adsorbents reached equilibrium within 120 minutes, with the adsorption process best described by the pseudo-second-order kinetic model. Thermodynamic analysis revealed an endothermic and spontaneous adsorption process. The superior performance of MAC in OM removal has significant implications for uranium extraction from phosphoric acid. By more efficiently removing organic contaminants, MAC prepares the phosphoric acid for subsequent uranium recovery processes, potentially leading to substantial enhancements in the economics of uranium recovery from this critical source for the nuclear fuel cycle. Moreover, the utilization of waste tires as a precursor for these effective adsorbents addresses environmental concerns related to tire disposal while providing a cost-effective solution for phosphoric acid purification. This approach aligns with circular economy principles, turning a waste product into a valuable resource for the nuclear and phosphate industries.

REFERENCES

Abderrahim, N., Mergbi, M., Ben Amor, H., Djellabi, R., 2023. Optimization of microwave assisted synthesis of activated carbon from biomass waste for sustainable industrial crude wet-phosphoric acid purification. J. Clean. Prod. 136326. https://doi.org/10.1016/J.JCLEPRO.2023.136326

Ali, M.M., Attia, A.A., Taha, M.H., El-Maadawy, M.M., Abo-Raia, A.M., Abouria, A., 2019. Application of Acid Activated Bentonite for Efficient Removal of Organic Pollutants from Industrial Phosphoric Acid: Kinetic and Thermodynamic Study. SPE Middle East Oil Gas Show Conf. MEOS, Proc. 2019-March. https://doi.org/10.2118/194719-MS

Ania, C.O., Menéndez, J.A., Parra, J.B., Pis, J.J., 2004. Microwave-induced regeneration of activated carbons polluted with phenol. A comparison with conventional thermal regeneration. Carbon N. Y. 42, 1383–1387. https://doi.org/10.1016/J.CARBON.2004.01.010

Aoudia, K., Azem, S., Aït Hocine, N., Gratton, M., Pettarin, V., Seghar, S., 2017. Recycling of waste tire rubber: Microwave devulcanization and incorporation in a thermoset resin. Waste Manag. 60, 471–481. https://doi.org/10.1016/J.WASMAN.2016.10.051

Awwad, N.S., El-Nadi, Y.A., Hamed, M.M., 2013. Successive processes for purification and extraction of phosphoric acid produced by wet process. Chem.

Eng. Process. Process Intensif. 74, 69–74. https://doi.org/10.1016/J.CEP.2012.11.009

Azizian, S., Eris, S., 2021. Adsorption isotherms and kinetics. Interface Sci. Technol. 33, 445–509. https://doi.org/10.1016/B978-0-12-818805-7.00011-4

Badr, M.M., Youssef, W.M., Elgammal, E.M., Abdel Hameed, R.S., El-Maadawy, M.M., Hussien, A.E.M., 2023. Investigating the efficiency of bisphenol-A diglycidyl ether/resole phenol formaldehyde/polyamine blends as Cerium adsorbent from aqueous solution. J. Environ. Chem. Eng. 11. https://doi.org/10.1016/j.jece.2023.111475

Beltrami, D., Chagnes, A., Haddad, M., Laureano, H., Mokhtari, H., Courtaud, B., Jugé, S., Cote, G., 2013. Development of New Cationic Exchangers for the Recovery of Uranium (VI) from Concentrated Phosphoric Acid. Sep. Sci. Technol. 48, 480–486. https://doi.org/10.1080/01496395.2012.703752

Boulkroune, N., Meniai, A.H., 2012. Modeling Purification of Phosphoric Acid Contaminated with Cadmium by Liquid-liquid Extraction. Energy Procedia 18, 1189–1198. https://doi.org/10.1016/J.EGYPRO.2012.05.134

Chailuecha, C., Klinbumrung, A., Chaopanich, P., Sirirak, R., 2021. Graphene-like porous carbon nanostructure from corn husk: Synthesis and characterization. Mater. Today Proc. 47, 3525–3528. https://doi.org/10.1016/J.MATPR.2021.03.512

Chaudhuri, B., Ghosh, S., Mondal, B., Bhadra, D., 2022. Preparation and characterization of carbon fibre powder (CFP)-polyvinyl alcohol (PVA) composite films showing percolation threshold behaviour. Mater. Sci. Eng. B 275, 115500. https://doi.org/10.1016/J.MSEB.2021.115500

Colomba, A., Berruti, F., Briens, C., 2022. Model for the physical activation of biochar to activated carbon. J. Anal. Appl. Pyrolysis 168, 105769. https://doi.org/10.1016/J.JAAP.2022.105769

Cordova Estrada, A.K., Cordova Lozano, F., Lara Díaz, R.A., 2021. Thermodynamics and Kinetic Studies for the Adsorption Process of Methyl Orange by Magnetic Activated Carbons. https://doi.org/10.1177/1178622211013336 14. https://doi.org/10.1177/1178622211013336

Doke, K.M., Khan, E.M., 2012. Adsorption thermodynamics to clean up wastewater; critical review. Rev. Environ. Sci. Bio/Technology 2012 121 12, 25–44. https://doi.org/10.1007/S11157-

012-9273-Z

El-Maadawy, M.M., 2024. Enhanced uranium removal from leach liquor using raw and activated sludge as sustainable adsorbents. Int. J. Environ. Anal. Chem. https://doi.org/10.1080/03067319.2024.2352652

El-Maadawy, M.M., 2019. HDEHP-Impregnated Kaolinite for Adsorption of Uranium from Dilute Phosphoric Acid. Radiochem. 2019 613 61, 331–338. https://doi.org/10.1134/S1066362219030081

El-Maadawy, M.M., Elzoghby, A.A., Masoud, A.M., El-Deeb, Z.M., El Naggar, A.M.A., Taha, M.H., 2024a. Conversion of carbon black recovered from waste tires into activated carbon via chemical/microwave methods for efficient removal of heavy metal ions from wastewater. RSC Adv. 14, 6324–6338. https://doi.org/10.1039/D4RA00172A

El Naggar, A.M.A., Ali, M.M., Abdel Maksoud, S.A., Taha, M.H., Morshedy, A.S., Elzoghby, A.A., 2019. Waste generated bio-char supported co-nanoparticles of nickel and cobalt oxides for efficient adsorption of uranium and organic pollutants from industrial phosphoric acid. J. Radioanal. Nucl. Chem. 320, 741–755. https://doi.org/10.1007/S10967-019-06529-2/TABLES/3

Elgohary, D.M., El-Sabbagh, S.M., Mira, H.I., Desouky, O.A., Hussien, S.S., El Naggar, A.M.A., Ali, A.O., El-Maadawy, M.M., 2024. Chemical modification of Aspergillus flavus extracted chitosan for uranium remediation from aqueous solution. Int. J. Environ. Anal. Chem. https://doi.org/10.1080/03067319.2024.2358420

Fang, K., Xu, L., Yang, M., Chen, Q., 2023. One-step wet-process phosphoric acid by-product CaSO4 and its purification. Sep. Purif. Technol. 309, 123048. https://doi.org/10.1016/J.SEPPUR.2022.123048

Fawzy, M.M., Farag, N.M., Amin, A.S., 2018. Treatment of Crude Phosphoric Acid from Some Undesirable Impurities. J. Basic Environ. Sci. 5, 204–216.

Forouzesh, M., Fatehifar, E., Khoshbouy, R., Daryani, M., 2023. Experimental investigation of iron removal from wet phosphoric acid through chemical precipitation process. Chem. Eng. Res. Des. 189, 308–318.

González, M.P., Navarro, R., Saucedo, I., Avila, M., Revilla, J., Bouchard, C., 2002. Purification of phosphoric acid solutions by reverse osmosis and nanofiltration. Desalination 147, 315–320. https://doi.org/10.1016/S0011-9164(02)00558-1

Gupta, V.K., Nayak, A., Agarwal, S., Tyagi, I., 2014. Potential of activated carbon from waste

rubber tire for the adsorption of phenolics: effect of pre-treatment conditions. J. Colloid Interface Sci. 417, 420–430. https://doi.org/10.1016/J.JCIS.2013.11.067

Hamza, W., Chtara, C., Benzina, M., 2013. Retention of organic matter contained in industrial phosphoric acid solution by raw Tunisian clays: Kinetic equilibrium study. J. Chem. 2013. https://doi.org/10.1155/2013/218786

Hamza, W., Fakhfakh, N., Dammak, N., Belhadjltaeif, H., Benzina, M., 2020. Sono-assisted adsorption of organic compounds contained in industrial solution on iron nanoparticles supported on clay: Optimization using central composite design. Ultrason. Sonochem. 67, 105134. https://doi.org/10.1016/J.ULTSONCH.2020.105134

Heidarinejad, Z., Dehghani, M.H., Heidari, M., Javedan, G., Ali, I., Sillanpää, M., 2020. Methods for preparation and activation of activated carbon: a review. Environ. Chem. Lett. 2020 182 18, 393–415. https://doi.org/10.1007/S10311-019-00955-0

Ibrahim, S., Masoud, A.M., El-Maadawy, M.M., Fahmy, H., Taha, M., 2024. Recycling waste polymer packaging materials as effective active carbon porous materials for uranium removal from commercial phosphoric acid. Radiochim. Acta 112, 95–109. https://doi.org/10.1515/RACT-2023-0165/HTML

Ibrahim, S.A., Masoud, A.M., Taha, M.H., Meawad, A.S., 2021. New organic compounds detection and potential removal in crude phosphoric acid using waste sludge. https://doi.org/10.1080/03067319.2021.1959564. https://doi.org/10.1080/03067319.2021.1959564

Jiang, H., Shao, J., Zhu, Y., Yu, J., Cheng, W., Yang, H., Zhang, X., Chen, H., 2023. Production mechanism of high-quality carbon black from high-temperature pyrolysis of waste tire. J. Hazard. Mater. 443, 130350. https://doi.org/10.1016/J.JHAZMAT.2022.130350

Jin, X., Wu, X., Zhang, H., Jiang, X., Huang, Z., Liu, Y., Fang, M., Min, X., 2018. Novel humic acid-based carbon materials: adsorption thermodynamics and kinetics for cadmium(II) ions. Colloid Polym. Sci. 296, 537–546. https://doi.org/10.1007/S00396-018-4271-5/FIGURES/8

Jjagwe, J., Olupot, P.W., Menya, E., Kalibbala, H.M., 2021. Synthesis and Application of Granular Activated Carbon from Biomass Waste Materials for Water Treatment: A Review. J. Bioresour. Bioprod. 6, 292–322.

https://doi.org/10.1016/J.JOBAB.2021.03.003

Joseph, C.G., Krishniah, D., Taufiq-Yap, Y.H., Massuanna, M., William, J., 2015. Preparation and Characterization of Activated Carbon from Waste Rubber Tires: A Comparison between Physical and Chemical Activation. Adv. Mater. Res. 1107, 347–352. https://doi.org/10.4028/WWW.SCIENTIFIC.NET/AMR.1107.347

Kouzbour, S., Gourich, B., Gros, F., Vial, C., Allam, F., Stiriba, Y., 2019. Comparative analysis of industrial processes for cadmium removal from phosphoric acid: A review. Hydrometallurgy 188, 222–247. https://doi.org/10.1016/J.HYDROMET.2019.06.014

Kouzbour, S., Gourich, B., Gros, F., Vial, C., Stiriba, Y., 2022. Purification of industrial wet phosphoric acid solution by sulfide precipitation in batch and continuous modes: Performance analysis, kinetic modeling, and precipitate characterization. J. Clean. Prod. 380, 135072. https://doi.org/10.1016/J.JCLEPRO.2022.135072

Largitte, L., Pasquier, R., 2016. A review of the kinetics adsorption models and their application to the adsorption of lead by an activated carbon. Chem. Eng. Res. Des. 109, 495. https://doi.org/10.1016/j.cherd.2016.02.006

Lewandowski, W.M., Januszewicz, K., Kosakowski, W., 2019. Efficiency and proportions of waste tyre pyrolysis products depending on the reactor type—A review. J. Anal. Appl. Pyrolysis 140, 25–53. https://doi.org/10.1016/J.JAAP.2019.03.018

Leydier, A., Arrachart, G., Turgis, R., Bernier, G., Marie, C., Miguirditchian, M., Pellet-Rostaing, S., 2017. Recovery of uranium (VI) from concentrated phosphoric acid using bifunctional reagents. Hydrometallurgy 171, 262–266. https://doi.org/10.1016/j.hydromet.2017.05.008

Li, L., Liu, S., Zhu, T., 2010. Application of activated carbon derived from scrap tires for adsorption of Rhodamine B. J. Environ. Sci. 22, 1273–1280. https://doi.org/10.1016/S1001-0742(09)60250-3

Liu, F., Wang, H., Xue, L., Fan, L., Zhu, Z., 2008. Effect of microstructure on the mechanical properties of PAN-based carbon fibers during high-temperature graphitization. J. Mater. Sci. 43, 4316–4322. https://doi.org/10.1007/S10853-008-2633-Y/FIGURES/13

Liu, X., Wu, F., Qu, G., Jin, C., Liu, Y., Kuang, L., Li, H., Chen, X., Wang, Z., Cheng, Y., 2022. Application prospect of advanced oxidation technology in wet process phosphoric acid production. J. Environ. Chem. Eng. 10, 108868. https://doi.org/10.1016/J.JECE.2

022.108868

Marszałek, M., Knapik, E., Piotrowski, M., Chruszcz-Lipska, K., 2023. Removal of cadmium from phosphoric acid in the presence of chloride ions using commercially available anion exchange resins. J. Ind. Eng. Chem. 118, 488–498. https://doi.org/10.1016/j.jiec.2022.11.032

Martínez, R.J., Vela-Carrillo, A.Z., Godínez, L.A., Pérez-Bueno, J. de J., Robles, I., 2023. Competitive adsorption of anionic and cationic molecules on three activated carbons derived from agroindustrial waste. Biomass and Bioenergy 168. https://doi.org/10.1016/j.biombioe.2022.106660

Masoud, A.M., El-Maadawy, M.M., Taha, M.H., Meawad, A., 2023. Uranium capture from aqueous solution using cement kiln dust; equilibrium and kinetic studies. J. Radioanal. Nucl. Chem. 332, 2487–2497. https://doi.org/10.1007/S10967-023-08937-X

Masoud, A.M., El-Maadawy, M.M., Taha, M.H., Younes, A.A., 2024. Dithiocarbamate functionalised crosslinked polyacrylamide for separation and pre-concentration of uranium (VI) ions from sulphate medium. Int. J. Environ. Anal. Chem. https://doi.org/10.1080/03067319.2024.2329314

Masoud, A. M., Saeed, M., Taha, M.H., El-Maadawy, M.M., 2020. Uranium adsorption from Bahariya Oasis leach liquor via TOPO impregnated bentonite material; Isothermal, kinetic and thermodynamic studies. Egypt. J. Chem. 63, 721–741. https://doi.org/10.21608/EJCHEM.2019.13638.1843

Mohamad Nor, N., Lau, L.C., Lee, K.T., Mohamed, A.R., 2013. Synthesis of activated carbon from lignocellulosic biomass and its applications in air pollution control—a review. J. Environ. Chem. Eng. 1, 658–666. https://doi.org/10.1016/J.JECE.2013.09.017

Morshedy, A.S., Taha, M.H., El-Aty, D.M.A., Bakry, A., El Naggar, A.M.A., 2021. Solid waste sub-driven acidic mesoporous activated carbon structures for efficient uranium capture through the treatment of industrial phosphoric acid. Environ. Technol. Innov. 21, 101363. https://doi.org/10.1016/J.ETI.2021.101363

Morsy, A., Taha, M.H., Saeed, M., Waseem, A., Riaz, M.A., Elmaadawy, M.M., 2019. Isothermal, kinetic, and thermodynamic studies for solid-phase extraction of uranium (VI) via hydrazine-impregnated carbon-based material as efficient adsorbent. Nucl. Sci. Tech. 30, 1–11. https://doi.org/10.1007/S41365-019-0686-Z/TABLES/5

Neolaka, Y.A.B., Riwu, A.A.P., Aigbe, U.O., Ukhurebor, K.E., Onyancha, R.B., Darmokoesoemo, H., Kusuma, H.S., 2023. Potential of activated carbon from various sources as a low-cost adsorbent to remove heavy metals and synthetic dyes. Results Chem. 5, 100711. https://doi.org/10.1016/J.RECHEM.2022.100711

Ondon, B.S., Sun, B., Yan, Z.Y., Zhu, X.M., Liu, H., 2014. Effect of microwave heating on the regeneration of modified activated carbons saturated with phenol. Appl. Water Sci. 4, 333–339. https://doi.org/10.1007/S13201-013-0147-5/FIGURES/8

Park, Y.G., Kim, K.T., 2021. Selective separation of various heavy metals from synthesized phosphoric acid solutions. J. Ind. Eng. Chem. 95, 267–276. https://doi.org/10.1016/J.JIEC.2020.12.032

Poursorkhabi, V., Abdelwahab, M.A., Misra, M., Khalil, H., Gharabaghi, B., Mohanty, A.K., 2020. Processing, Carbonization, and Characterization of Lignin Based Electrospun Carbon Fibers: A Review. Front. Energy Res. 8, 208. https://doi.org/10.3389/FENRG.2020.00208/BIBTEX

Qu, W., Liu, J., Xue, Y., Wang, X., Bai, X., 2018. Potential of producing carbon fiber from biorefinery corn stover lignin with high ash content. J. Appl. Polym. Sci. 135, 45736. https://doi.org/10.1002/APP.45736

Raimundo, R.A., Silva, V.D., Silva, T.R., Medeiros, E.S., Macedo, D.A., Gomes, U.U., Gomes, R.M., Morales, M.A., 2022. Synthesis and characterization of NiFe-carbon fibers by solution blow spinning and application for the oxygen evolution reaction. J. Phys. Chem. Solids 160, 110311. https://doi.org/10.1016/J.JPCS.2021.110311

Saleh, T.A., Gupta, V.K., Al-Saadi, A.A., 2013. Adsorption of lead ions from aqueous solution using porous carbon derived from rubber tires: Experimental and computational study. J. Colloid Interface Sci. 396, 264–269. https://doi.org/10.1016/J.JCIS.2013.01.037

Semião, A.J.C., Rossiter, H.M.A., Schäfer, A.I., 2010. Impact of organic matter and speciation on the behaviour of uranium in submerged ultrafiltration. J. Memb. Sci. 348, 174–180. https://doi.org/10.1016/J.MEMSCI.2009.10.056

Şenol, Z.M., Şimşek, S., 2020. Equilibrium, kinetics and thermodynamics of Pb(II) ions from aqueous solution by adsorption onto chitosan-dolomite composite beads. https://doi.org/10.1080/03067319.2020.1790546 1–15.

Shekhawat, A., Jugade, R., Gomase, V., Kahu, S., Dhandayutham, S., Pandey, S., 2023. Adsorptive

Removal of As(III) by Cellulose-Sn(IV) Biocomposite. J. Compos. Sci. 7, 19. https://doi.org/10.3390/JCS7010019

Sultana, M., Rownok, M.H., Sabrin, M., Rahaman, M.H., Alam, S.M.N., 2022. A review on experimental chemically modified activated carbon to enhance dye and heavy metals adsorption. Clean. Eng. Technol. 6, 100382. https://doi.org/10.1016/J.CLET.2021.100382

Taha, M.H., Abdel Maksoud, S.A., Ali, M.M., El Naggar, A.M.A., Morshedy, A.S., Elzoghby, A.A., 2019. Conversion of biomass residual to acid-modified bio-chars for efficient adsorption of organic pollutants from industrial phosphoric acid: an experimental, kinetic and thermodynamic study. https://doi.org/10.1080/03067319.2019.1618459 99, 1211–1234. https://doi.org/10.1080/03067319.2019.1618459

Taha, M.H., El-Maadawy, M.M., Hussein, A.E.M., Youssef, W.M., 2018. Uranium sorption from commercial phosphoric acid using kaolinite and metakaolinite. J. Radioanal. Nucl. Chem. 317, 685–699. https://doi.org/10.1007/S10967-018-5951-9/TABLES/5

Taha, S.M., Amer, M.E., Elmarsafy, A.E., Elkady, M.Y., 2014. Adsorption of 15 different pesticides on untreated and phosphoric acid treated biochar and charcoal from water. J. Environ. Chem. Eng. 2, 2013–2025. https://doi.org/10.1016/J.JECE.2014.09.001

Tan, K.L., Foo, K.Y., 2022. The viable role of activated carbon for the effective remediation of refinery and petrochemical wastewaters. Pet. Ind. Wastewater Adv. Sustain. Treat. Methods 185–203. https://doi.org/10.1016/B978-0-323-85884-7.00016-3

Thonglhueng, N., Sirisangsawang, R., Sukpancharoen, S., Phetyim, N., 2022. Optimization of iodine number of carbon black obtained from waste tire pyrolysis plant via response surface methodology. Heliyon 8, e11971. https://doi.org/10.1016/J.HELIYON.2022.E11971

Xu, S., He, R., Dong, C., Sun, N., Zhao, S., He, H., Yu, H., Zhang, Y.B., He, T., 2022. Acid stable layer-by-layer nanofiltration membranes for phosphoric acid purification. J. Memb. Sci. 644, 120090. https://doi.org/10.1016/J.MEMSCI.2021.120090

Youssef, W.M., El-Maadawy, M.M., Masoud, A.M., Alhindawy, I.G., Hussein, A.E.M., 2024. Uranium capture from aqueous solution using palm-waste based activated carbon: sorption kinetics and equilibrium. Environ. Monit. Assess. 196. https://doi.org/10.1007/S10661-

Youssef, W.M., Masoud, A.M., Elmaadawy, M.M., Khawassek, Y.M., 2024. Uranium (VI) sorption from aqueous solution using commercial anion exchange resins; kinetics, isotherm, and thermodynamic investigations. J. Radioanal. Nucl. Chem. 333, 1975–1989. https://doi.org/10.1007/S10967-024-09438-1

Youssef, W.M., Hussein, A.E.M., Taha, M.H., El-Maadawy, M.M., 2022. Uranium(VI) Sorption from Liquid Waste Solution Using Functionalized Polyurethane Polymer: Kinetic and Isotherm Characterizations. Russ. J. Inorg. Chem. 67, 1058–1068. https://doi.org/10.1134/S0036023622070245

024-12560-Y

تنقية فعالة لحمض الفوسفوريك الصناعي المركز باستخدام بقايا نفايات الإطارات الكربونية المنشطة بالميكروويف؛ دراسات ديناميكية الحركة والاتزان والديناميكا الحرارية

محمود المعداوي

تقيم هذه الدراسة إزالة المادة العضوية (OM) من حمض الفوسفوريك المركز كمعالجة أولية لعملية استخلاص اليورانيوم. حيث يتم تفحيم الإطارات المستعملة لإنتاج جزيئات الكربون الأسود (AC)، والتي يتم تنشيطها لاحقًا عن طريق المعالجة بالميكروويف (MAC). وقد تم توصيف كل من AC وMAC باستخدام FTIR وXRD وRaman spectrometry وSEM وBET. حيث أجريت تجارب امتصاص المادة العضوية في ظل الظروف المختلفة من تركيز حمض الفوسفوريك ووقت التلامس ودرجة الحرارة وجرعة المادة الماصة. وفي ظل الظروف المثلى (١٢٠ دقيقة، ١٥ جم/ لترمن المادة الماصة، ٤٣٪ P_2O_5، درجة حرارة الغرفة)، حقق AC أقصى سعة امتصاص تبلغ ٣٨.٤٦ مجم/جم، بينما وصلت MAC إلى ٤٧.٦٢ مجم/جم. وقد اتبعت حركية الامتزاز نموذج ثنائي الرتبة الكاذبة، مع ملاءمة بيانات التوازن لنموذج لانجمير. وقد أشار ايضا التحليل الديناميكي الحراري إلى ان العملية هي ماصة للحرارة وتلقائية وقابلة للتطبيق. وقد تساهم هذه الدراسة في تحسين كفاءة استعادة اليورانيوم من حمض الفوسفوريك من خلال معالجة المواد العضوية. حيث تعمل إزالة المواد العضوية باستخدام جزيئات الكربون المنشط بالميكروويف على تحضير حمض الفوسفوريك لاستخراج اليورانيوم بشكل أكثر فعالية، مما قد يؤدي إلى زيادة العائد والنقاء في مراحل الاستخلاص بالمذيبات اللاحقة، مع آثار كبيرة على دورة الوقود النووي والاستخدام المستدام لموارد الفوسفات.